5.6. Barrow, Alaska (01/13/14 – 11/28/14)

This section describes quality control of solar data recorded at Barrow between 01/13/14 – 11/28/14. A total of 17,249 scans of the SUV-100 spectroradiometer are part of the Barrow Volume 24 dataset.

Data of the SUV-100 spectroradiometer collected during the reporting period were affected by the following problems:

- Failure of the PID controller for controlling the monochromator temperature
  The proportional-integral-derivative (PID) controller that controls the heater of the monochromator failed on 4/28/14. It was replaced on 5/12/14. Monochromator temperatures during this period ranged between 30 and 32 °C. (The target tempertaure is 33 °C). The effect of the reduced temperature on the instrument's wavelength stability was negligible, however, comparisons with the GUV measurements suggested that solar data of the SUV-100 were to high by 2 - 5% during this period. Data were scaled down accordingly.
- Failure of system control unit ("Spectralink")
  Coincident with electrical work in the building where the instrument is located, the power supply and the board interfacing with the computer failed on 7/13/14. The components were replaced on 07/30/14. No data are available for the period 07/14/14 and 07/30/14 because of this problem. Of note, the system is equipped with an Uninterruptable Power Supply (UPS). Apparently the device was not able to protect the system from the power glitch resulting from the electrical work.

5.6.1. Irradiance Calibration

The site irradiance standards of the reporting period were the lamps M-699, 200W009, and 200W042, which were also used in 2012 and 2013.

Lamp 200W042 was calibrated in June 2007 at BSI with four 1000-Watt FEL lamps provided by the Central UV Calibration Facility (CUCF) at Boulder. This calibration procedure was complicated by the fact that the irradiance scale of the four FEL lamps refers to the detector-based scale of the National Institute of Standards and Technology established in 2000 (NIST2000; Yoon et al., 2002), whereas all solar data of the NSF UVSIMN refer to the source-based NIST scale from 1990 (NIST1990, Walker et al., 1987). The NIST2000 scale is about 1.3% larger than the NIST1990 scale. Data of certificates issued by CUCF were converted to the NIST1990 scale before the calibration was transferred to the site standard.

Lamps M-699 and 200W009 were originally calibrated by Optronic Laboratories (OL) in March 2001. Both lamps were brought to San Diego in 2007 and recalibrated against lamps 200W028 and 200W022. (Lamp 200W028 is the San Diego site standard; lamp 200W022 is BSI's long-term standard, which preserves the OL scale from March 2001.)

The three lamps were compared with the traveling standard 200W017 in June 2013. At this time, the calibrations of lamps 200W009 and 200W042 agreed to within ±1.0% with that of the traveling standard. The difference between the calibrations of lamp M-699 and the travelling standard was slightly worse but still within the range of the uncertainty of calibration standards.

The three on-site lamps were compared with each other on 2/28/14 and 9/29/14. The calibrations of lamps M-699 and 200W042 agreed with each other to within ±0.5% on both occasions. (See Figure 5.6.1 for results of the first cross-calibration event.) The calibration of lamp 200W009 deviated from that of the other two lamps by up to 3%. Additional analysis suggested that the output of lamp 200W009 was unstable throughout the reporting period and measurements of that lamp were therefore not used for the calibration of solar data.

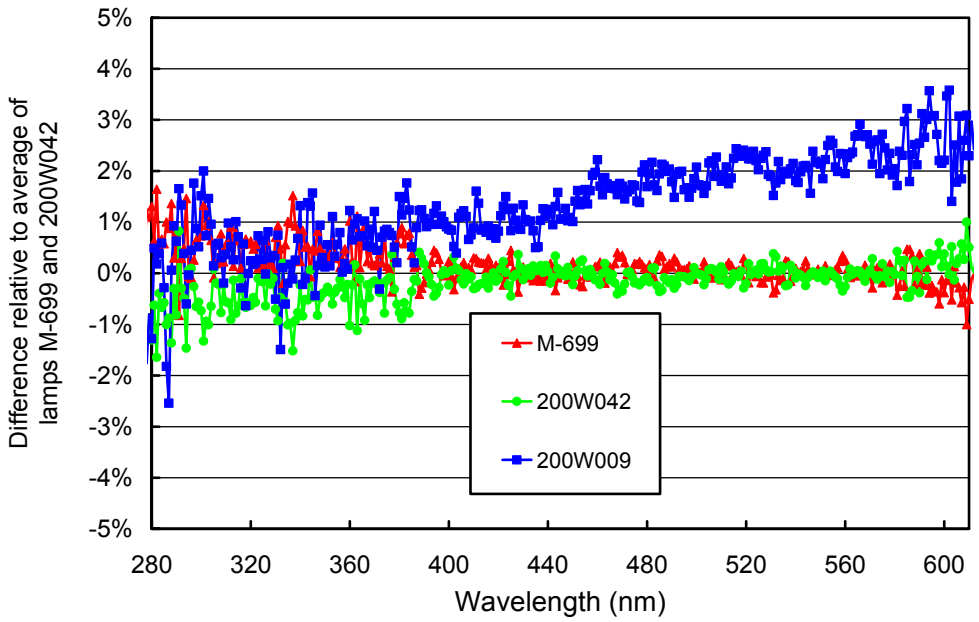

Figure 5.6.1. *Comparison of on-site lamps M-699, 200W042, and 200W009 on 2/28/14.*

5.6.2. Instrument Stability and Calibration

The radiometric stability of the SUV-100 spectroradiometer was monitored with calibrations utilizing the three site irradiance standards, daily "response" scans of the internal lamp, by comparison with measurements of the GUV-511 multifilter radiometer, and by comparisons with results of a radiative transfer model.

The stability of the internal lamp is monitored with the TSI sensor, which is independent from possible monochromator and PMT drifts. By logging the PMT currents at several wavelengths during response scans, changes in monochromator throughput and PMT sensitivity can be detected. Figure 5.6.2 shows changes in TSI readings and PMT currents at 300 and 400 nm, derived from response scans performed between 1/1/14 and 12/7/14. During this time, the output of the internal lamp as indicated by the TSI sensor decreased by less than 4.5% and this change is well reflected in the changes of the PMT currents, indicating that monochromator and PMT were stable.

Comparison of GUV and SUV measurements indicated that SUV solar data are too high between 4/28/14 and 5/11/14 when the temperature of the monochromator was abnormally low due to the failure of the PID controller. Unfortunately, no "absolute" calibration scans are available for this period. Based on the GUV/SUV comparison results, SUV data were scaled down by 6% at and below 305 nm, 4% at 320 nm, 3% at 340 and 380 nm, and 2% between 400 and 600 nm. The uncertainty of solar measurements is increased by 2% during this period.

The reporting period was broken down into 8 calibration periods established with calibrations using the on-site standards. Table 5.6.1 provides more information on these periods and Figure 5.6.3 shows the ratios of the irradiance assigned to the internal reference lamp in Periods P1B and P4 relative to that applied in Period P1.

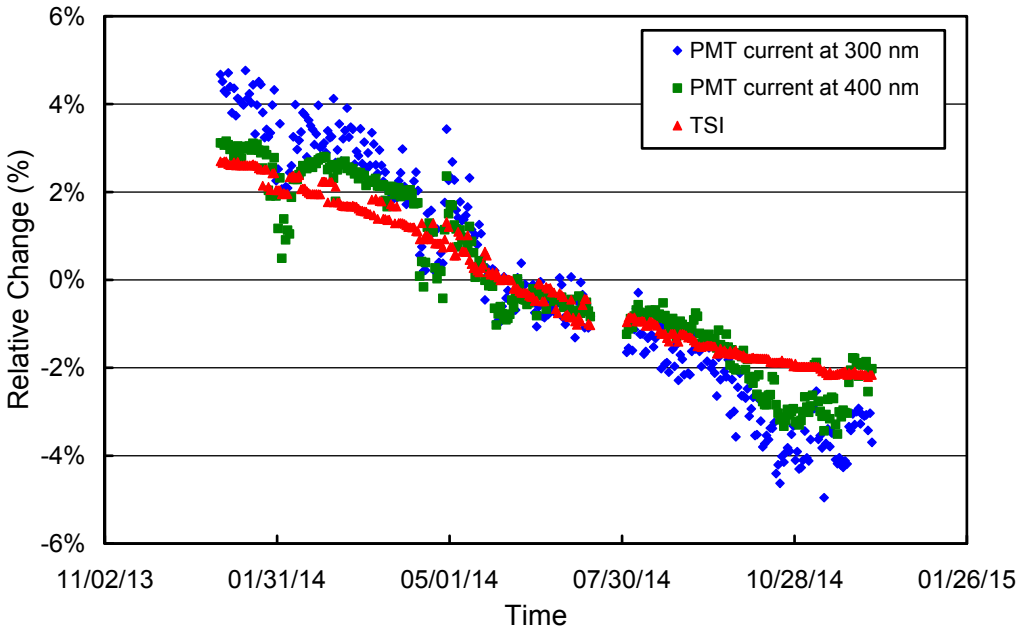

Figure 5.6.2. *Time-series of PMT current at 300 and 400 nm, and TSI signal. All data were extracted from measurements of the internal irradiance standard and are normalized to their average.*

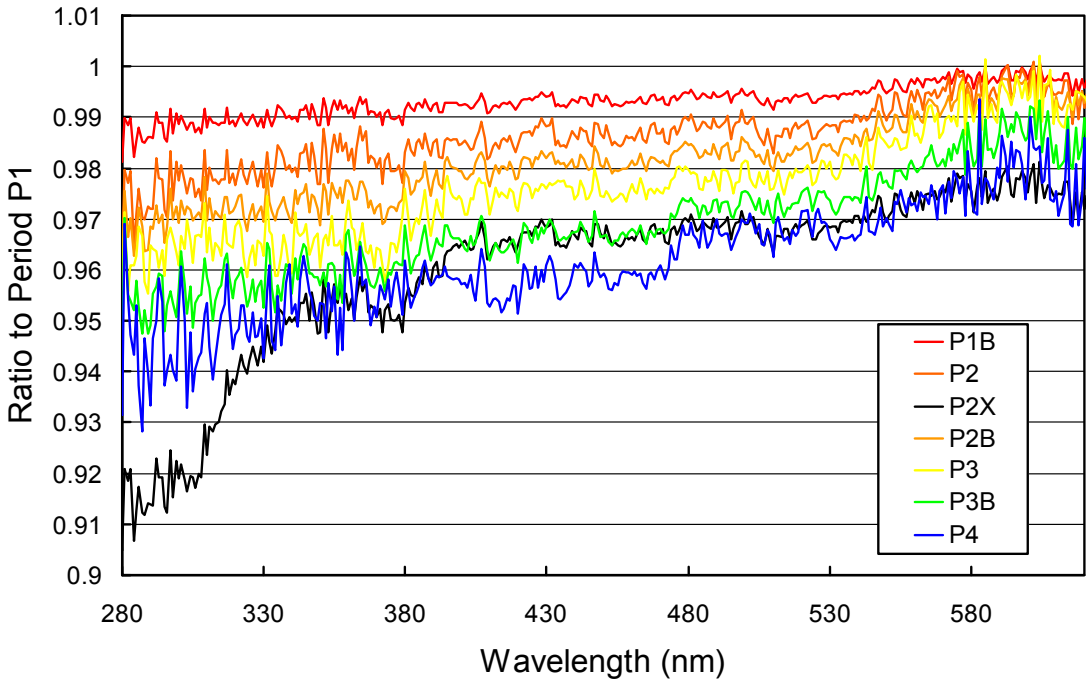

Figure 5.6.3. *Ratios of spectral irradiance assigned to the internal reference lamp during the Periods P1B – P4, relative to Period P1.*

Table 5.6.1. Calibration periods for Barrow Volumes 24.

Period name	Period range	Number of absolute scans	Remarks
P1	01/01/14 - 03/19/14	4	
P1B	03/20/14 - 03/30/14		Average of Periods P1 and P2
P2	03/31/14 - 4/27/14 and 05/12/14 - 09/01/14	4	
P2X	04/28/14 - 05/11/14		Period P2, scaled as explained in text
P2B	09/02/14 - 09/25/14		Average of Periods P2 and P3
P3	09/26/14 - 10/02/14	2	
P3B	10/03/14 - 10/17/14		Average of Periods P3 and P4
P4	10/18/14 - 12/31/14	1	

Figure 5.6.4 presents ratios of standard deviation and average spectra, calculated from individual absolute scans performed in each calibration period. These ratios are useful for estimating the variability of calibrations assigned to each period. The variability is less than 1.5% for the three periods.

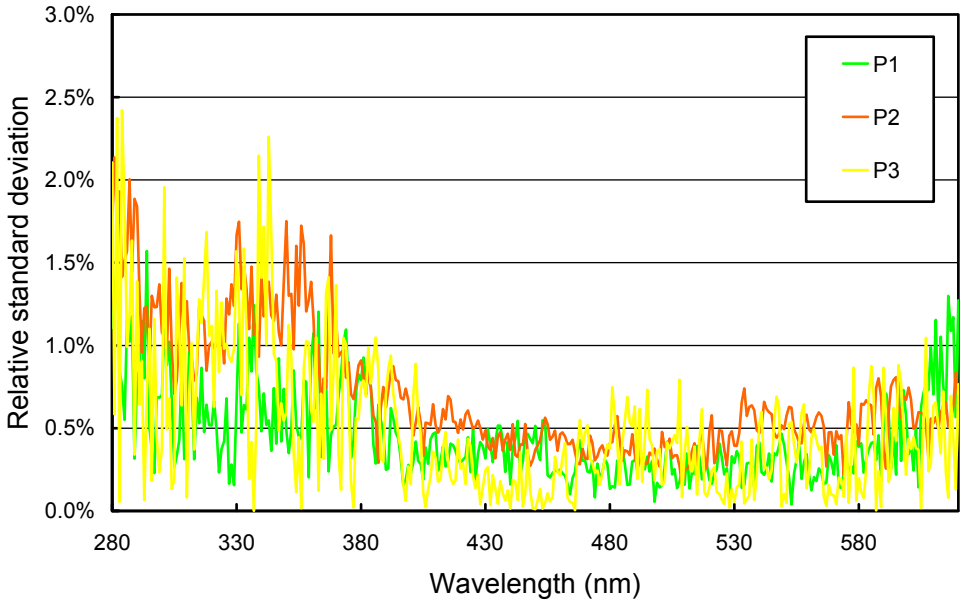

Figure 5.6.4. *Ratio of standard deviation and average spectra calculated from irradiance spectra applied to the internal lamp.*

SUV-100 data were also compared to measurements of the collocated GUV-511 radiometer. The ratio of GUV and SUV data at 320 nm as a function of time is shown in Figure 5.6.5. The standard deviation of the ratio is 0.032. Variability is generally smaller in spring than fall because of less influence by clouds. The GUV/SUV ratio shows several step changes and short periods with systematic (i.e., non-random) difference from one.

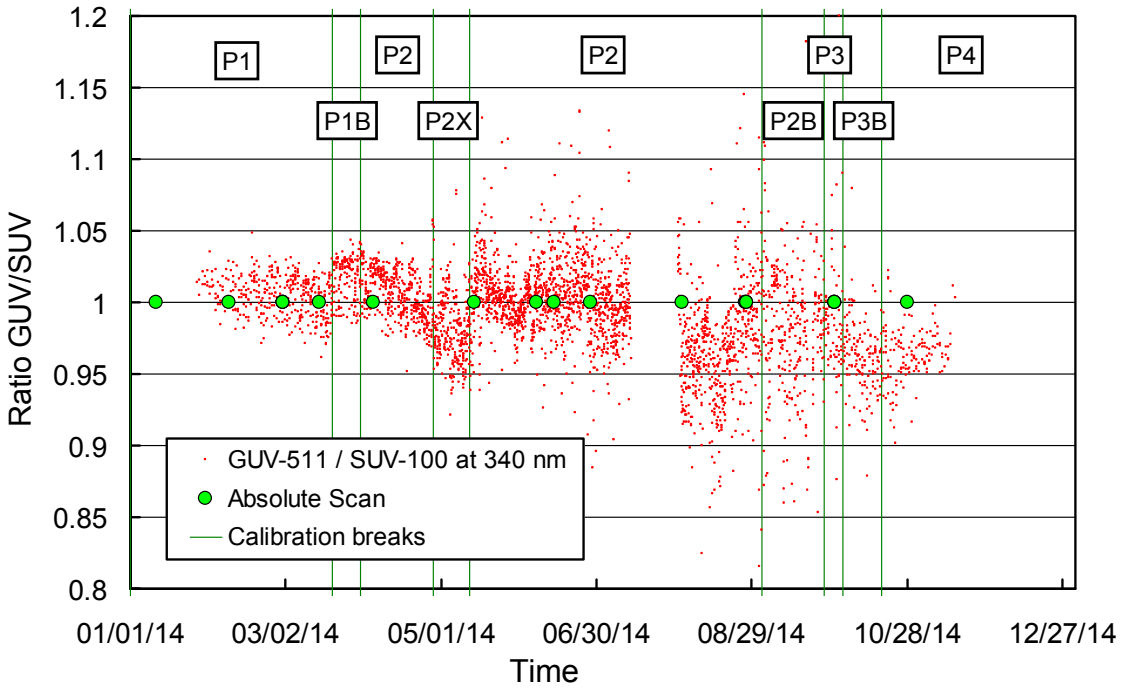

Figure 5.6.5. *Ratio of GUV-511 measurements of the 340-nm channel to SUV-100 measurements. The latter were weighted with the spectral response function of the 340-nm GUV-511 channel. Times of absolute scans and calibration breaks are also indicated.*

As a last check of data quality, SUV-100 measurements were compared with radiative transfer calculations. These calculations are part of Version 2 processing (uv.biospherical.com/ NSF/Version2/). The ratio of measured and modeled data was generally within the range observed in past years.

5.6.3. Wavelength Calibration

Wavelength stability of the system was monitored with the internal mercury lamp. Information from the daily wavelength scans was used to homogenize the data set by correcting day-to-day fluctuations in the wavelength offset. Figure 5.6.6 shows the differences in the wavelength offset of the 296.73 nm mercury line between two consecutive wavelength scans. A total 397 pairs, measured between 1/1/14 and 12/02/14, were evaluated. The change in offset was smaller than ±0.055 nm in 99% of all cases.

The function used to correct the non-linearity of the monochromator's wavelength drive is shown in Figure 5.6.7. It was calculated with the Version 2 Fraunhofer line correlation method (*Bernhard et al.*, 2004). Data were corrected with these functions and again tested with the correlation method. Results for four wavelengths in the UV and one in the visible are shown in Figure 5.6.8. Residual shifts in the UV are typically smaller than ±0.05 nm. The average standard deviation for all wavelengths between 310 and 590 nm is 0.030 nm. The wavelength accuracy of the Version 2 data set is slightly better. For example, the bias of about -0.07 nm indicated in the 360 nm measured between 9/22/14 and 11/6/14 has been reduced.

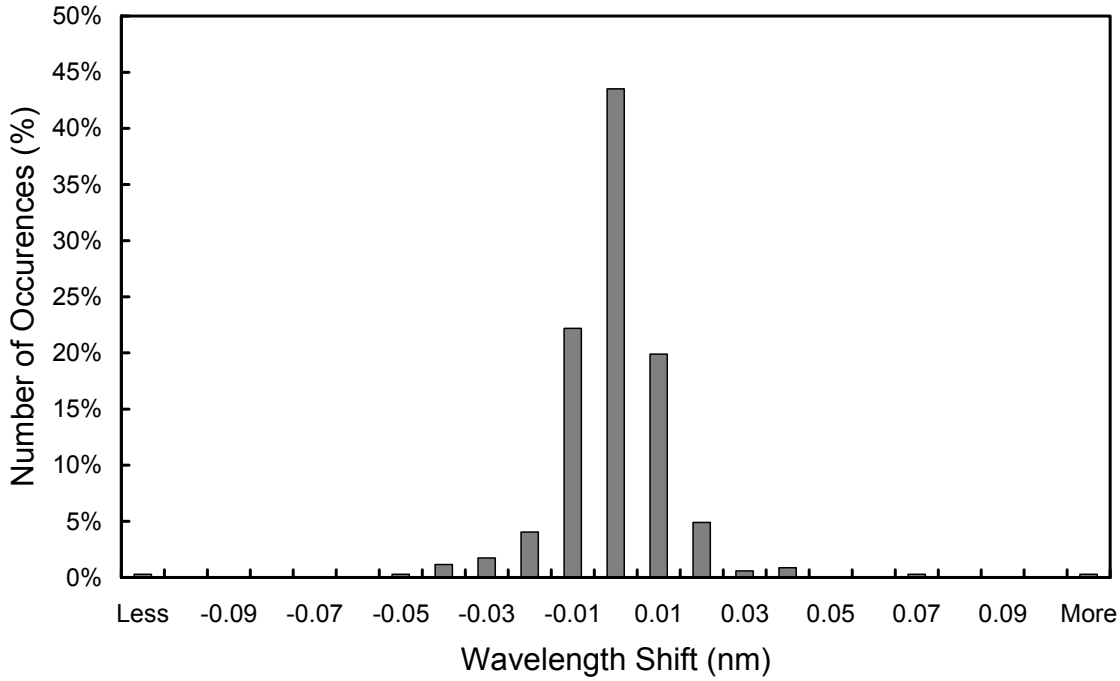

Figure 5.6.6. *Differences in the measured position of the 296.73 nm mercury line between consecutive wavelength scans. The x-labels give the center wavelength shift for each column. Thus the 0-nm histogram column covers the range -0.005 to +0.005 nm. "Less" means shifts smaller than –0.105 nm; "more" means shifts larger than 0.105 nm.*

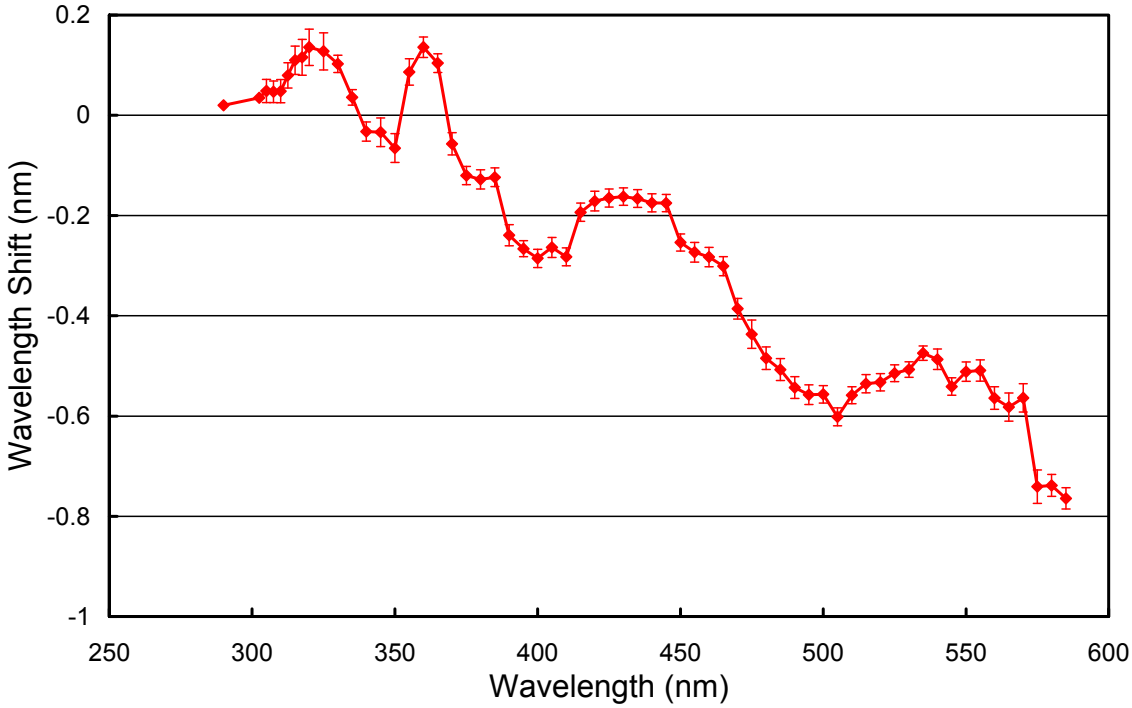

Figure 5.6.7. *Monochromator non-linearity correction function for Barrow Volume 24. Error bars indicate the standard deviation of the data contributing to this plot.*

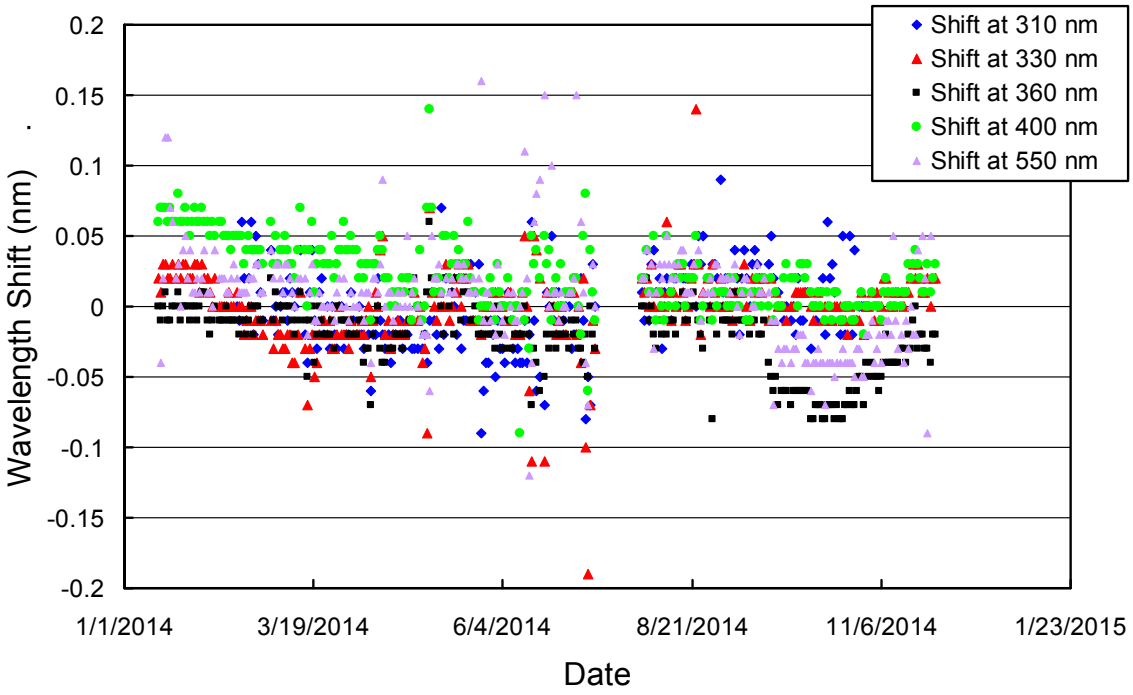

Figure 5.6.8. *Wavelength accuracy check of final data at four wavelengths in the UV and one in the visible by means of Fraunhofer-line correlation. The noontime measurement has been evaluated for each day of the reporting period when the Sun was above the horizon. The vertical black line marks the time of the site visit.*

5.6.4. Missing Data

A total of 17,249 scans are part of the Barrow Volume 24 dataset (01/13/14 – 11/28/14). There are no data for the periods 7/14/14 – 7/30/14 because of the failure of the system's interface board. There are also no data for 9/20/14 due to a planned power outage.

5.6.5. GUV Data

The GUV-511 radiometer installed next to the SUV-100 was calibrated against final SUV-100 measurements following the procedure outlined in Section 4.3.1. Data products were calculated from calibrated measurements (Section 4.3.2). Figure 5.6.9. shows a comparison of SUV-100 and GUV-511 erythemal irradiance based on final Volume 24 data. The bias between the two instruments depends somewhat on season. Some of the seasonality is caused by the simplifications of the GUV inversion procedure. Measurements of the GUV's 305 nm channel are close to the detection limit when SZA exceeds 75° and the total ozone column is large. The large noise in GUV data during those conditions also affects the calculation of secondary data products such as erythemal irradiance. We advise data users to use SUV-100 rather than GUV-511 data, in particular when the SZA exceeds 75°. For SZAs < 75°, the median ratio SUV/GUV is 1.011.

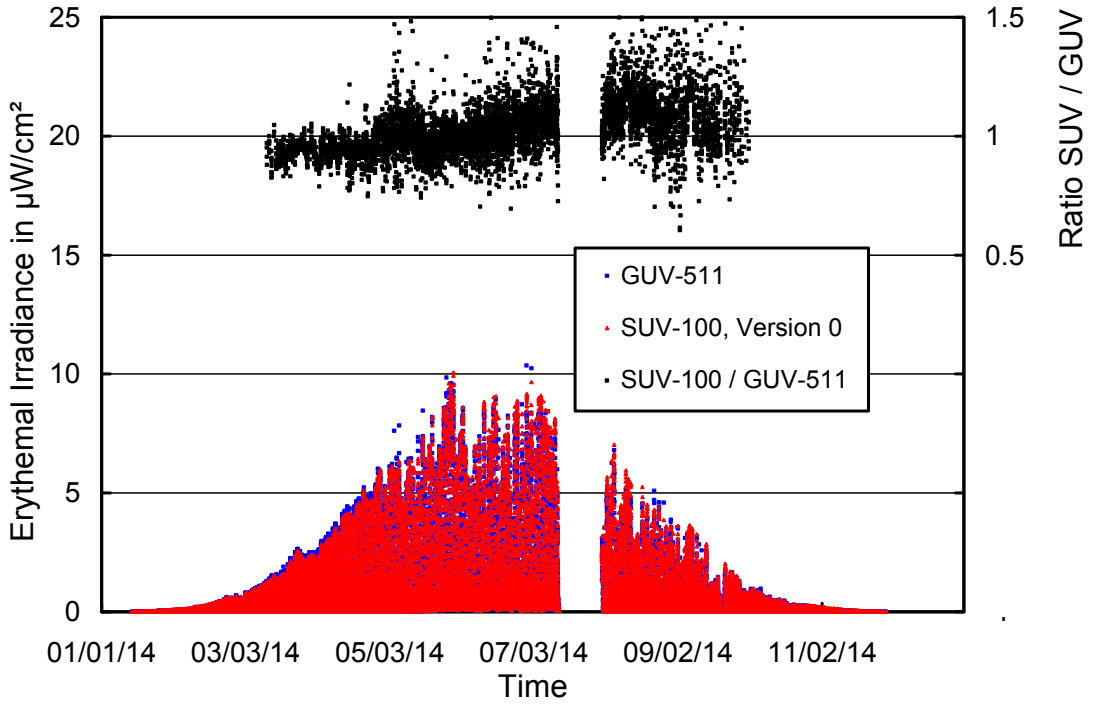

Figure 5.6.9. *Comparison of erythemal irradiance measured by the SUV-100 spectroradiometer and the GUV-511 radiometer. Data are based on "Version 0" (cosine-error uncorrected) data.*

Figure 5.6.10 shows a comparison of total ozone measurements from the GUV-511, the Ozone Monitoring Instrument (OMI) on NASA's AURA satellite (Version 8.5, Collection 3), and the SUV-100 (Version 2 data using climatological profiles with temperature correction). GUV-511 ozone values were calculated as described in Section 4.3.3. GUV-511 data measured between 3/12/14 and 10/1/14 are on average 0.6% larger than OMI observations. For SZAs larger than 75°, GUV-511 ozone data become unreliable and should not be used. SUV-100 ozone data exceed OMI measurements on average by 2.5%. For more information on total ozone calculation from SUV-data at Barrow see *Bernhard et al*. (2003). The effect of the vertical distribution of ozone has been further discussed by *Bernhard et al*. (2005).

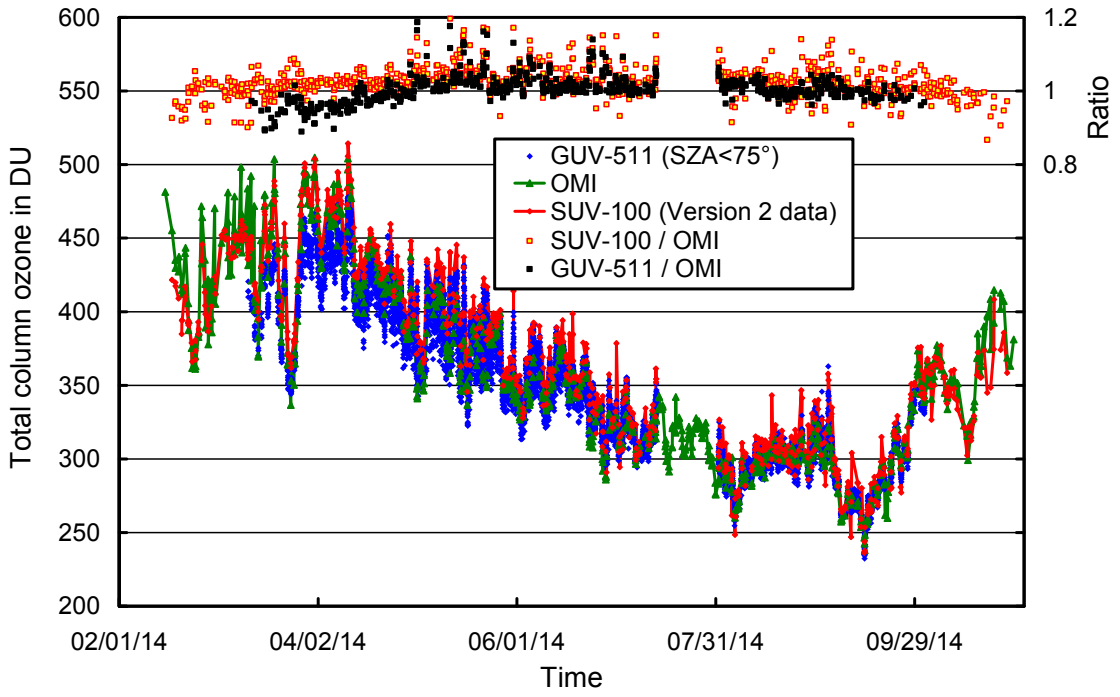

Figure 5.6.10. *Comparison of total column ozone measurements from GUV-511, OMI, and SUV-100. GUV-511 measurements are plotted in 30 minute intervals. For calculating the ratios of SUV-100/OMI and GUV-511/OMI, only measurements concurrent with the OMI overpass were evaluated.*

References

Bernhard, G., C.R. Booth, and R.D. McPeters. (2003). Calculation of total column ozone from global UV spectra at high latitudes. J. Geophys Research, 108(D17), 4532, doi:10.1029/2003JD003450.

Bernhard, G., C. R. Booth, and J. C. Ehramjian. (2004). Version 2 data of the National Science Foundation's Ultraviolet Radiation Monitoring Network: South Pole, J. Geophys. Res., 109, D21207, doi:10.1029/2004JD004937.

Bernhard, G., R.D. Evans, G.J. Labow, and S.J. Oltmans. (2005). Bias in Dobson Total Ozone Measurements at High Latitudes due to Approximations in Calculations of Ozone Absorption Coefficients and Airmass. J. Geophys. Res., 110, D10305, doi:10.1029/2004JD005559.

Bernhard, G., C. R. Booth, J. C. Ehramjian, R. Stone, and E. G. Dutton. (2007), Ultraviolet and visible radiation at Barrow, Alaska: Climatology and influencing factors on the basis of version 2 National Science Foundation network data, J. Geophys. Res., 112, D09101, doi:10.1029/2006JD007865.

Walker, J.H., R.D. Saunders, J.K. Jackson, and D.A. McSparron. (1987). Spectral Irradiance Calibrations. NBS Special Publication 250-20, U.S. Dept. of Commerce, National Bureau of Standards, Washington, DC, 37 pp., plus appendices.

Yoon H.W., C.E. Gibson, and P.Y. Barnes. (2002). Realization of the National Institute of Standards and Technology detector-based spectral irradiance scale. Appl. Opt., 41(28), 5,879-5,890.